

# Multidimensional Dynamic Experiments for Data-Rich Process Development of Reactions in Flow

## **Supporting Information**

### **Table of Contents**

Analytical Method: .....	3
Materials:.....	3
Reaction Automation:.....	4
Residence Time Distribution (RTD) – Experiments .....	5
Multidimensional Nonlinear Dynamic Experiments .....	8
1-Dimensional Sine Experiments (constant $\tau$ ) .....	8
Comparison between linear and nonlinear dynamic experiments.....	8
Model Regression .....	9

### **Table of Figures**

<b>Fig. S1</b> Representative HPLC chromatogram used in the analysis of the Knoevenagel condensation.....	3
<b>Fig. S2</b> LabVIEW generated user interface (top) and state machine code (bottom) used to conduct the dynamic experiments. ....	5
<b>Fig. S3</b> Residence time distribution results in the form an F-curve for the 0.5 (left) and 10 (right) minute residence time conditions explored. The UV (top plots) and HPLC (bottom plots) results are both included. 6	6
<b>Fig. S4</b> Optimized fits of the experimental data (red circles) to the $E_{\theta}$ function found in Levenspiel (black lines) for the (A) 0.5-minute and (B) 10-minute nominal residence time cases. ....	6
<b>Fig. S5</b> Optimized fit of the experimental data (red circles) to the well-known $E_{\theta}$ function found in Levenspiel (black lines) for the 10-minute nominal residence time case after employing a Savitzky-Golay differential filter and an 11-point smoothing array.....	7
<b>Fig. S6</b> Inputs and results from the 1-dimensional sine wave experiment. (A) Input DBU equivalents profile and anticipated DBU equivalents in the outlet corrected for the 5-minute residence time. (B) Measured DBU equivalents (as determined by internal standards) in the sample fractions as a function of experimental time. (C) <i>p</i> -Anisaldehyde and product concentration as a function experimental time. (D) <i>p</i> -Anisaldehyde and product concentration as a function of measured DBU equivalents. (E) Product concentration imposed against the design space, where the blue and black data points represent data from the linear and nonlinear (sine profile) dynamic experiments, respectively. ....	8
<b>Fig. S7</b> Comparison of the results from linear (black) and nonlinear (red) dynamic experiments. (A) Design space illustrating the span of conditions studied in both cases. (B,C,D,E) Various views of the reaction profile data superimposed above the design space.....	9
<b>Fig. S8</b> Residuals of the cubic model fit to the compiled dataset illustrated in (A) 3D and (B) 2D with color representing the absolute value of the residuals. ....	10

**Fig. S9** Results from the regression of a single 2-dimensional nonlinear dynamic experiment against the cubic function. (A) Model fit superimposed against the experimental data. (B) Contour plot generated using the model fit. (C,D) Residuals from the fit. ....10

### **Table of Tables**

**Table S1** Coefficient values and statistical results from the regression of *all* experimental data against a cubic equation. ....9

**Table S2** Coefficient values and statistical results from the regression of the 2-dimensional nonlinear (30 min gradient) experimental data against a cubic equation. ....11

## Analytical Method:

Prior to analysis, a 10  $\mu\text{L}$  aliquot was sampled from each fraction collected and diluted with 1 mL of pure acetonitrile. The samples were analyzed on an Agilent 1290 Infinity II using an Agilent ZORBAX Eclipse Plus C18 (50 mm x 4.6 mm, 1.8  $\mu\text{m}$  particle size). An analytical method was developed for compound separation utilizing 0.1%  $\text{H}_3\text{PO}_4$  (by volume) in water and acetonitrile as Mobile Phase A and B, respectively. The column temperature, flow rate, injection volume, and UV detection wavelength used are 25°C, 1.0 mL/min, 5.0  $\mu\text{L}$ , and 220 nm, respectively. The mobile phase composition (Mobile Phase A:B) is held constant at 70:30 for 1 minute, then shifted to 5:95 over 5.5 minutes and held for 1 minute before reverting back to 70:30. The HPLC was calibrated by injecting known standards of *p*-anisaldehyde and (4-methoxybenzylidene) malononitrile, the reactant and product, respectively. A representative HPLC spectrum is shown in Fig. S1 along with the identity of the peaks.

The acetonitrile was purchased from Fisher (Optima® LC/MS grade, 0.1 micron filtered) and used as is. Water was also purchased from Fisher (Optima® LC/MS, 0.03 micron filtered) and used as is. *o*-Phosphoric acid was purchased from Fisher (Certified ACS, 85%) and used as is.

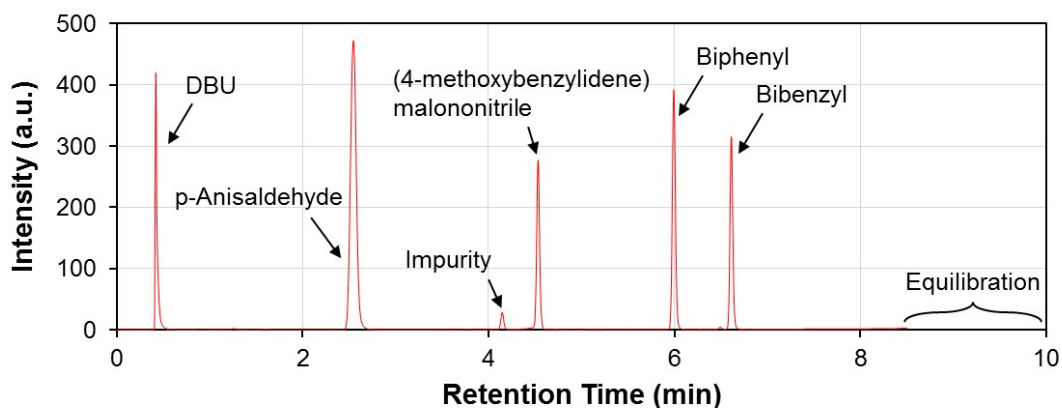


Fig. S1 Representative HPLC chromatogram used in the analysis of the Knoevenagel condensation.

Internal standards, biphenyl and bibenzyl, were used to normalize HPLC results and to establish DBU equivalents relative to the starting material, *p*-anisaldehyde. For each experiment, the starting materials and base streams were calibrated to establish a calibration “ratio” between biphenyl and bibenzyl. Knowing the concentration of the starting material and base streams, a biphenyl:bibenzyl ratio (via area counts at 220 nm) can be established for a known DBU equivalents. To accomplish this, 5  $\mu\text{L}$  each of the starting materials and base streams were combined and diluted with 1 mL acetonitrile and analyzed via HPLC. This volume ratio, given the 0.5 M and 0.2 M concentrations of the starting materials and base streams, respectively, corresponds to 0.4 eq. DBU. The actual DBU equivalents experienced in each fraction sample can be calculated using Eq. (S1) below. This relationship is helpful to ensure the accuracy of the conditions tested and for evaluating flowrate consistency.

$$\text{Eq}_{\text{DBU Actual, } i} = \frac{0.4 \text{ eq.}}{\left(\frac{A_{\text{Biphenyl}}}{A_{\text{Bibenzyl}}}\right)_{\text{Calibration}}} \left[ \left(\frac{A_{\text{Biphenyl}}}{A_{\text{Bibenzyl}}}\right)_{i, \text{ Experimental}} \right] \quad (\text{S1})$$

## Materials:

*p*-Anisaldehyde was ordered from Acros Organics (Reagent grade, 99+%) and used as is. Malononitrile was ordered from Aldrich ( $\geq 99\%$ ) and used as is. 1,8-Diazabicyclo[5.4.0]undec-7-ene (DBU) was purchased from Sigma-Aldrich (Puriss. grade,  $\geq 99.0\%$  by GC) and used as is. Trifluoroacetic acid (TFA) was purchased from Sigma-Aldrich (Reagent grade, 99%) and used as is. The biphenyl and bibenzyl internal standards were purchased from Sigma-

Aldrich ( $\geq 99\%$ ) and Sigma-Aldrich (ReagentPlus<sup>®</sup>, 99%), respectively, and used as is. Acetonitrile was purchased from Fisher (Optima<sup>®</sup> LC/MS grade, 0.1 micron filtered) and used as is.

New stock solutions were prepared on the day of each experiment. To prepare the 0.5 M starting materials stock solution, approximately 13.62 g of biphenyl and 27.23 g of *p*-anisaldehyde were added to a 200 mL volumetric flask. Acetonitrile solvent was added to achieve a total volume of 200 mL. Approximately 13.21 g of malononitrile was added to a separate 200 mL volumetric flask and diluted to 200 mL with acetonitrile solvent. These streams were mixed immediately prior to the experiment in a Wheaton bottle for use. To prepare the 0.2 M base solution, approximately 12.18 g of DBU and 13.62 g of bibenzyl were added to a 200 mL volumetric flask and diluted to 200 mL with acetonitrile solvent. This solution was mixed with 200 mL of pure acetonitrile in a Wheaton bottle for use. The 1.0 M TFA quench solution was prepared by diluting approximately 57.01 g of TFA to 1000 mL with acetonitrile solvent in a 1 L volumetric flask. This solution was transferred to a Wheaton bottle for use. Acetonitrile solvent (~500 mL) was added to a Wheaton bottle for use as is.

### Reaction Automation:

The reactor platform was automated using LabVIEW (National Instruments, 2017 SPI Full Developer Suite) with a state machine template architecture available from JKI, a third-party software company. The JKI state machine architecture employs an event structure within a case structure within a while loop, where states are queued and executed in order. This structure is very versatile, allowing for excellent user interface (UI) development, programmatic execution when necessary, and asynchronous loop signals to repeatedly queue states. This is ideal for a reactor system requiring user inputs and continuous manipulation of equipment inputs while recording equipment outputs.

Using the JKI template, states were created within the case structure for each instrument (Knauer pumps, fraction collector, Flow IR via OPC UA connectivity, and analytical balances) defined to complete individual tasks, such as setting pump flowrates, reading pump pressures, and fraction collector sampling commands. These states are then sent to the queue using user-events, either initiated by the user directly via the UI or using asynchronous loop triggers. Using multiple asynchronous loops, various states can be continuously added to the queue at differing time-intervals. As it pertains to the dynamic reaction platform, for example, a prompt on the UI starts the experiment and sends a series of states to the queue. An asynchronous loop then queues states to record time and process variables. Using this automation, an experiment can be started and run seamlessly without the need for user intervention. Once the experiment is completed, the recorded process data, FTIR trends, and fractions are reviewed and analyzed off-line.

A snapshot of the LabVIEW generated user interface and code are provided in **Fig. S2**.

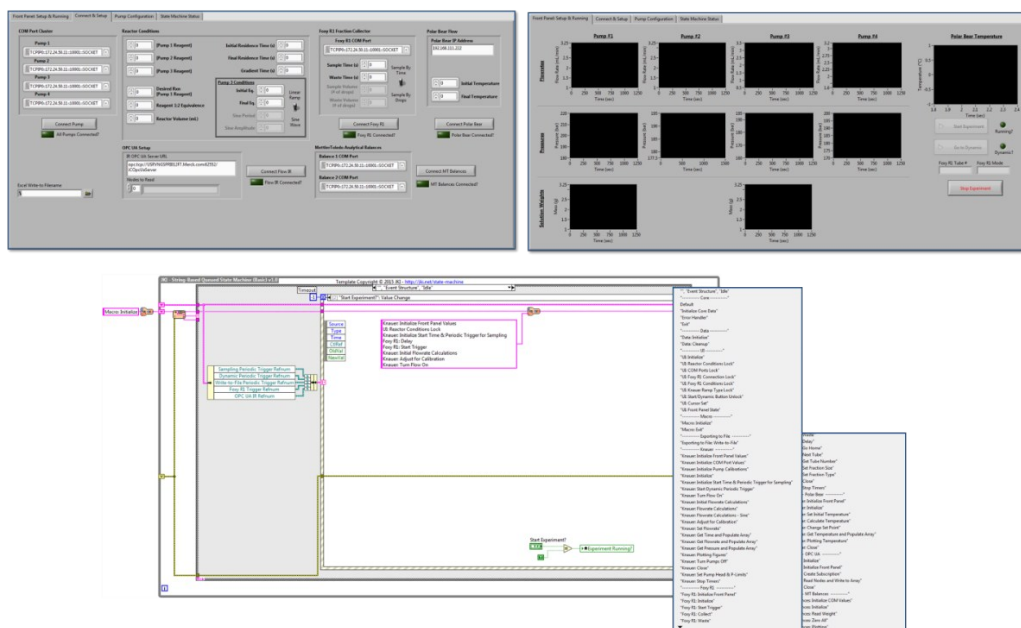


**Fig. S2** LabVIEW generated user interface (top) and state machine code (bottom) used to conduct the dynamic experiments.

## **Residence Time Distribution (RTD) – Experiments**

The residence time distribution in the flow reactor was investigated experimentally to determine if dispersion influenced the accuracy in correlating experimental data with reaction conditions. The experimental data was regressed against well-known dispersion models [O. Levenspiel. *Chemical Reaction Engineering*, John Wiley & Sons, Inc., New York, ed. 3, 1999] to calculate the dispersion number,  $D/uL$ , of the reactor under the specific operating conditions. The dispersion number is a metric of how far the reactor deviates from an ideal plug flow reactor. Dispersion numbers that approach zero are indicative of plug flow behavior while ones that approach infinity indicate mixed flow dynamics.

To perform these RTD experiments, step input changes were used to alter the concentration of toluene in acetonitrile at nominal residence times of 0.5 and 10 minutes; practically speaking, this was accomplished by changing the relative flowrates of pure acetonitrile and a mixture of toluene in acetonitrile while maintaining a constant overall flowrate. The downstream dispersion of this step change was analyzed using in-line UV detection (235 nm) and off-line HPLC analysis of fractions collected every 10 seconds, appropriately chosen to imitate the sampling time used for the reaction experiments. To conduct an experiment, a stream containing 2% toluene in acetonitrile was initially mixed with a stream of pure acetonitrile in a 1:3 ratio (2% Toluene/MeCN : pure MeCN). After system equilibration, the pump flowrates were changed to achieve a 3:1 ratio of 2% Toluene/MeCN to pure acetonitrile. After a time-period equivalent to the nominal residence time,  $\tau$ , the step change was observed. For all RTD experiments, the flowrate of the “quench” stream matched that used in the reaction experiments, though pure acetonitrile replaced the 1.0 M TFA solution typically used. Additionally, all RTD experiments were conducted with the reactor immersed in a water bath held at approximately 40°C.

The results obtained from both UV and HPLC analyses were transformed into the form of an F-curve taken by normalizing absorbance from 0 to 1 as a function of time. It is important to note that, at the shortest residence time (highest flowrate) where dispersion is highest, very little impact of dispersion is observed in the sampling fractions analyzed by HPLC (**Fig. S3**, bottom left), the method of analysis for all of the reaction results reported in the manuscript.

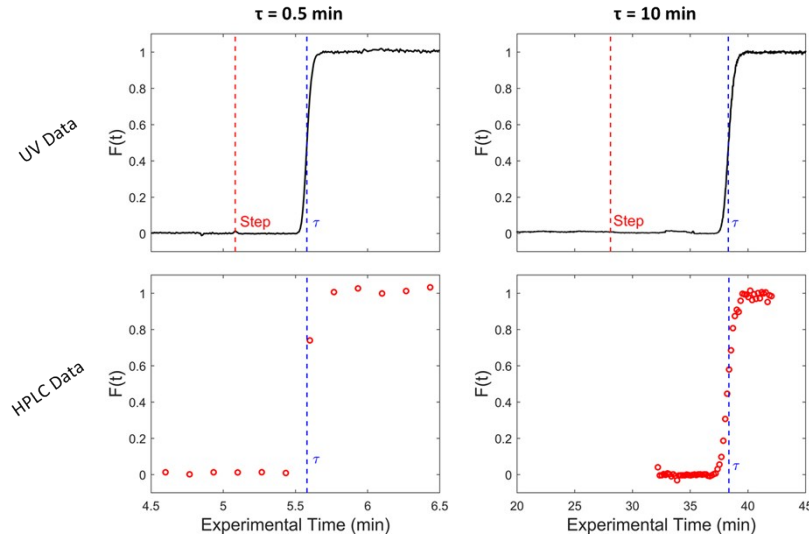


**Fig. S3** Residence time distribution results in the form of an F-curve for the 0.5 (left) and 10 (right) minute residence time conditions explored. The UV (top plots) and HPLC (bottom plots) results are both included.

Typically, however, RTD analysis is performed using an E-curve, obtained by taking the time-derivative of an F-curve. Here, the E-curve is computed via finite differences with the UV data and plotted in the form of an  $E(t/\tau)$  curve, where time is normalized to the mean (nominal) residence time. Based on the shape of the E-curve, the experimental data was fit to the residence time distribution model given in Eq. S2 using the *nlinfit* regression function in Matlab (**Fig. S4**) [O. Levenspiel. *Chemical Reaction Engineering*, John Wiley & Sons, Inc., New York, ed. 3, 1999]. The regressed values for mean residence time and dispersion coefficient are provided in text within the figures. The expected nominal residence times based on flowrates and reactor volume for the 0.5-minute and 10-minute RTD experiments were 0.5214 and 10.43 minutes, respectively, which are close to the regressed values.

$$E_{\theta} = \frac{1}{\sqrt{4\pi\left(\frac{D}{uL}\right)}} e^{-\frac{(1-\theta)^2}{4\left(\frac{D}{uL}\right)}} \quad \text{for } \frac{D}{uL} < 0.01 \quad (S2) \quad \theta = \frac{t}{\tau}$$

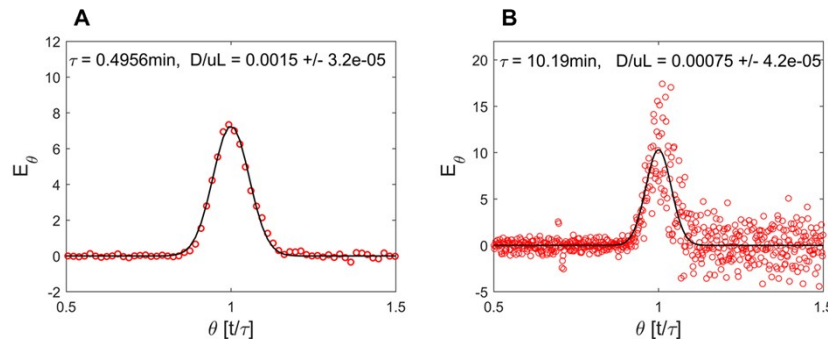


**Fig. S4** Optimized fits of the experimental data (red circles) to the  $E_{\theta}$  function found in Levenspiel (black lines) for the (A) 0.5-minute and (B) 10-minute nominal residence time cases.

Of note, the baseline noise in the resulting E-curve is significantly larger for the experimental data from the 10-minute relative to the 0.5-minute nominal residence time. This is a by-product of using the finite difference method to calculate the time-derivative of the experimental data. Despite the tighter peak shape of the  $E(t/\tau)$  curve in the 10-minute case, the step change spans a 2-minute timeframe around the nominal residence time

compared to the 6-second span observed for the 0.5-minute nominal residence time case. As such, the absolute value of the derivative is significantly larger for the 0.5-minute case, such that the signal-to-noise ratio is much greater.

One option for improving the signal-to-noise ratio for the 10-minute nominal residence time case is to apply an appropriate filtering technique, such as the Savitzky-Golay filter. This digital filter operates similar to a weighted moving average, but instead uses a convolution operation and fits a subset of the experimental data, known as a smoothing array, to a polynomial [A. Savitzky and M. J. E. Golay, *Analytical Chemistry*, **1964**, *36*, 1627-1639]. By using the convolution operation, signal features (e.g., peaks) are retained after filtering the data. The 10-minute data was filtered using a differential Savitzky-Golay filter with an 11-point smoothing array (e.g., the data point +/- 5 points) (shown in **Fig. S5**) and the regression results compared to those shown in **Fig. S4**. After filtering, the regressed nominal residence time and dispersion coefficient match quite closely ( $\tau = 10.19$  min,  $D/uL = 0.00075$  for unfiltered vs.  $\tau = 10.23$  min,  $D/uL = 0.00076$  for S-G filtered). The 0.5-minute nominal residence time RTD data did not require similar data filtering.

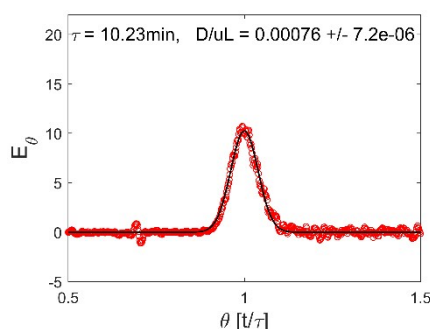


**Fig. S5** Optimized fit of the experimental data (red circles) to the well-known  $E_0$  function found in Levenspiel (black lines) for the 10-minute nominal residence time case after employing a Savitzky-Golay differential filter and an 11-point smoothing array.

According to Levenspiel, the reactor exhibits plug flow behavior when  $D/uL < 0.01$ . Based on the optimized fits, the dispersion number ( $D/uL$ ) in the experiments performed in this work ranged from  $7.5 \cdot 10^{-4}$  to  $1.5 \cdot 10^{-3}$ . Therefore, the assumption that the reactor behaves in a plugged flow manner is justified over the conditions explored for this application.

## **Multidimensional Nonlinear Dynamic Experiments**

### **1-Dimensional Sine Experiments (constant $\tau$ )**

Prior to the 2-dimensional nonlinear dynamic experiments, the sine profile in DBU equivalents was tested while the residence time was held constant ( $\tau = 5$  minutes). Results of this experiment (shown in **Fig. S6**) indicate that the platform can generate a sine wave profile accurately and the reaction concentration results closely match those obtained by using a linear gradient (see **Fig. S6E**). As shown in **Fig. S6D**, the reaction profiles overlay well indicating good internal repeatability. It is important to note that no additional information is obtained when operating a 1-dimensional dynamic experiment in a nonlinear fashion relative to a linear gradient. Improvements in efficiency and data density are only realized when employing nonlinear profiles in 2-dimensional dynamic experiments.

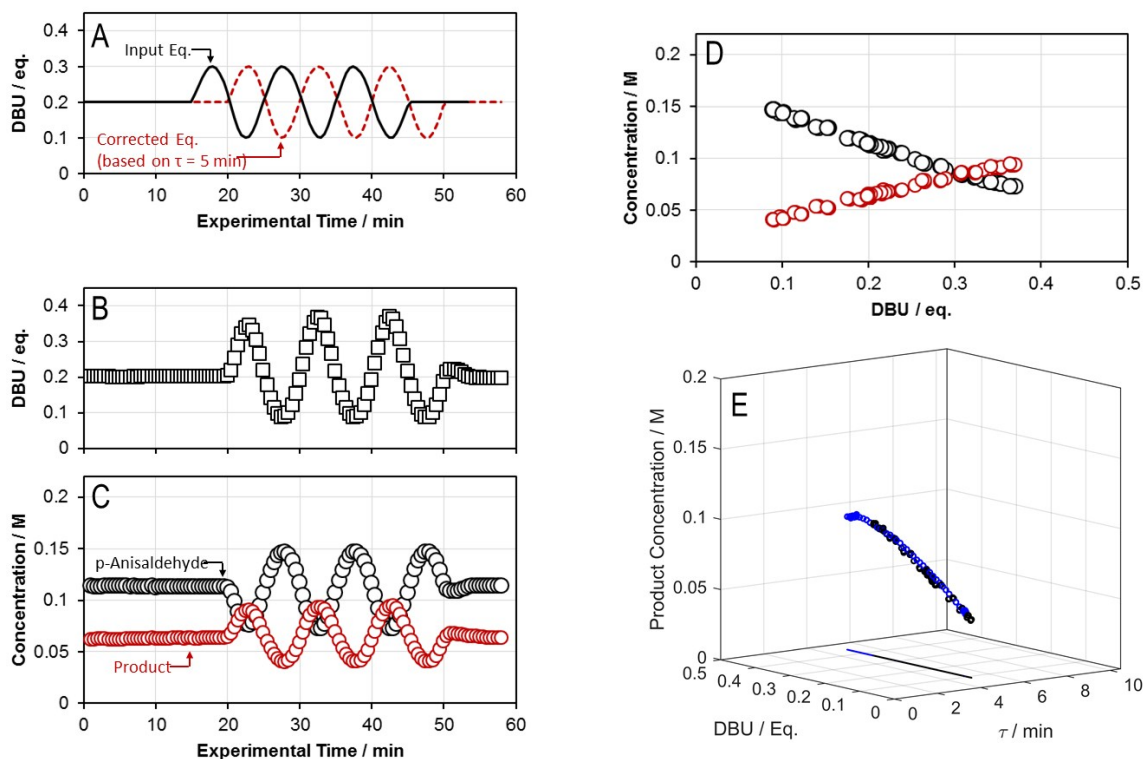


**Fig. S6** Inputs and results from the 1-dimensional sine wave experiment. (A) Input DBU equivalents profile and anticipated DBU equivalents in the outlet corrected for the 5-minute residence time. (B) Measured DBU equivalents (as determined by internal standards) in the sample fractions as a function of experimental time. (C) *p*-Anisaldehyde and product concentration as a function of experimental time. (D) *p*-Anisaldehyde and product concentration as a function of measured DBU equivalents. (E) Product concentration imposed against the design space, where the blue and black data points represent data from the linear and nonlinear (sine profile) dynamic experiments, respectively.

### Comparison between linear and nonlinear dynamic experiments

One of the principal arguments of this work surrounds the efficiency gains obtained by multidimensional linear and, more so, by nonlinear dynamic experiments. The efficiency gains from employing nonlinear dynamic experiments are best illustrated by **Fig. S7**. A single 2-dimensional experiment, employing a nonlinear profile in DBU equivalents and linear ramp in residence time (**Fig. S7**, red curve), exhibits significantly greater coverage of the design space throughout the experiment than any one of the linear 1- or 2-dimensional dynamic experiments performed. In fact, the nonlinear dynamic experiment provides a comparable dataset to all five linear dynamic experiments shown in **Fig. S7** (black curves). Furthermore, by adjusting the experimental conditions, such as the sine period and amplitude and gradient time, coverage of the design space can be further optimized.

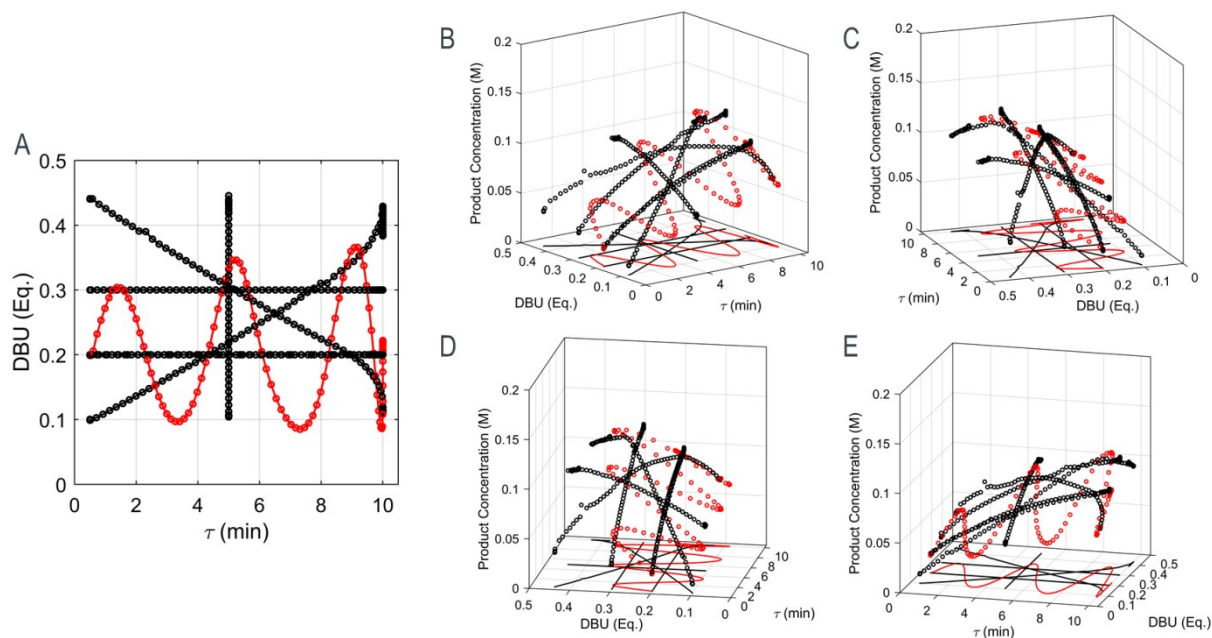


**Fig. S7** Comparison of the results from linear (black) and nonlinear (red) dynamic experiments. (A) Design space illustrating the span of conditions studied in both cases. (B,C,D,E) Various views of the reaction profile data superimposed above the design space.

## Model Regression

The compiled reaction data were regressed against a cubic function of the form shown in Eq. (S3) to generate a reaction model, where  $x$  and  $y$  represent DBU equivalents and residence time.

$$C_p = A + Bx + Cy + Dx^2 + Exy + Fy^2 + Gx^3 + Hx^2y + Ixy^2 + Jy^3 \quad (S3)$$

The estimated coefficients  $A$  through  $J$  are reported in **Table S1** along with the standard error,  $t$  statistic, and  $p$ -values reported by Matlab following the regression.

**Table S1** Coefficient values and statistical results from the regression of *all* experimental data against a cubic equation.

Coefficient	Estimated Value	Standard Error	$t$ Statistic	$p$ -Value
A	0.013984	0.0009239	15.137	6.6E-46
B	0.074252	0.0042890	17.312	1.4E-57
C	-0.023605	0.0052624	-4.4856	8.3E-06
D	-0.049571	0.0096961	-5.1125	3.9E-07
E	0.22336	0.0076837	29.069	8.1E-129
F	0.15898	0.0110180	14.429	2.7E-42
G	0.022572	0.0062616	3.6048	3.3E-04
H	-0.095235	0.0046956	-20.282	1.2E-74
I	-0.12302	0.0052180	-23.575	1.5E-94
J	-0.1124	0.0071539	-15.711	6.5E-49

The resulting fit from the regression plotted against the experiments results along with a contour plot detailing the product concentration response as a function of DBU equivalents and residence time are provided in the main

text. The residuals from the fit are shown in **Fig. S8**, both in 3- and 2-dimensions. These results show that the residuals are well distributed throughout the dataset indicating the absence of any systematic bias. Of note, residuals were highest for the 60 min sine wave experiment at the peaks of the DBU sine wave.

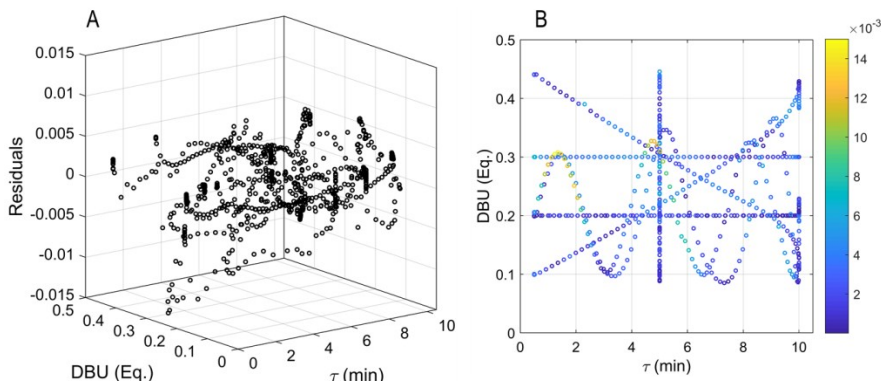


**Fig. S8** Residuals of the cubic model fit to the compiled dataset illustrated in (A) 3D and (B) 2D with color representing the absolute value of the residuals.

As mentioned in the main text, a single 2-dimensional nonlinear dynamic experiment provides sufficient information, spanning multiple conditions in the design space, to generate a reaction model. To prove this, the data from only the nonlinear dynamic experiment with a 30 min gradient was regressed against the cubic function, Eq. (S3). The results of this regression are shown in **Fig. S9**.

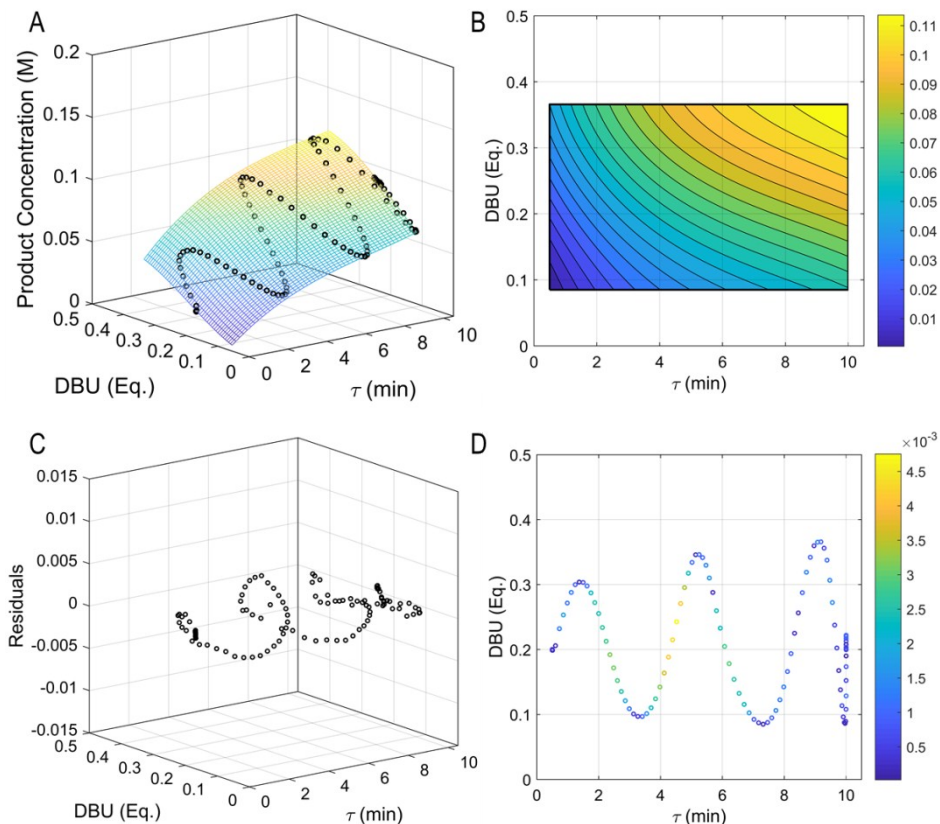


**Fig. S9** Results from the regression of a single 2-dimensional nonlinear dynamic experiment against the cubic function. (A) Model fit superimposed against the experimental data. (B) Contour plot generated using the model fit. (C,D) Residuals from the fit.

The model fit agrees well with the experimental data and the resultant contour plot matches the trends observed when fitting against the entire dataset. The residuals appear to follow a pattern through the design space. This is believed to be the result of weighting issues within the fit. There is a larger data density at the peaks and troughs of the sine wave relative to the middle of the range (~0.2 eq.). Thus, the residuals are lower at the peaks and troughs relative to these midpoints. By weighting the data accordingly, the model fit can be optimized.

The coefficient values and statistics resulting from the regression are shown in **Table S2**.

**Table S2** Coefficient values and statistical results from the regression of the 2-dimensional nonlinear (30 min gradient) experimental data against a cubic equation.

Coefficient	Estimated Value	Standard Error	<i>t</i> Statistic	<i>p</i> -Value
A	0.0005629	0.0021775	0.25851	0.79652
B	0.12815	0.0087402	14.662	3.7042e-27
C	0.031032	0.0092015	3.3725	0.0010439
D	-0.11778	0.014133	-8.3341	3.2225e-13
E	0.060654	0.014389	4.2152	5.2981e-5
F	0.044589	0.015382	2.8988	0.0045618
G	0.051097	0.0080505	6.347	5.6845e-9
H	-0.028322	0.0084448	-3.3538	0.0011097
I	-0.020286	0.0089117	-2.2764	0.024853
J	-0.030438	0.010297	-2.956	0.0038486